

EVALUATING THE PERFORMANCE OF NVIDIA'S A100 AMPERE GPU FOR SPARSE LINEAR ALGEBRA COMPUTATIONS

PREPRINT, COMPILED AUGUST 20, 2020

Yuhsiang Mike Tsai
Karlsruhe Institute of Technology,
Germany
yu-hsian.tsai@kit.edu

Terry Cojean
Karlsruhe Institute of Technology,
Germany
terry.cojean@kit.edu

Hartwig Anzt
Karlsruhe Institute of Technology,
Germany
University of Tennessee, Knoxville,
USA
hartwig.anzt@kit.edu

ABSTRACT

GPU accelerators have become an important backbone for scientific high performance computing, and the performance advances obtained from adopting new GPU hardware are significant. In this paper we take a first look at NVIDIA's newest server line GPU, the A100 architecture part of the Ampere generation. Specifically, we assess its performance for sparse linear algebra operations that form the backbone of many scientific applications and assess the performance improvements over its predecessor.

Keywords Sparse Linear Algebra · Sparse Matrix Vector Product · NVIDIA A100 GPU

1 INTRODUCTION

Over the last decade, Graphic Processing Units (GPUs) have seen an increasing adoption in high performance computing platforms, and in the June 2020 TOP500 list, more than half of the fastest 10 systems feature GPU accelerators [1]. At the same time, the June 2020 edition of the TOP500 is the first edition listing a system equipped with NVIDIA's new A100 GPU, the HPC line GPU of the Ampere generation. As the scientific high performance computing community anticipates this GPU to be the new flagship architecture in NVIDIA's hardware portfolio, we take a look at the performance we achieve on the A100 for sparse linear algebra operations.

Specifically, we first benchmark in Section 2 the bandwidth of the A100 GPU for memory-bound vector operations and compare against NVIDIA's A100 predecessor, the V100 GPU. In Section 3, we review the sparse matrix vector product (SpMV), a central kernel for sparse linear algebra, and outline the processing strategy used in some popular kernel realizations. In Section 4, we evaluate the performance of SpMV kernels on the A100 GPU for more than 2,800 matrices available in the Suite Sparse Matrix Collection [22]. The SpMV kernels we consider in this performance evaluation are taken from NVIDIA's latest release of the cuSPARSE library and the Ginkgo linear algebra library [2]. In Section 5, we compare the performance of the A100 against its predecessor for complete Krylov solver iterations that are popular methods for iterative sparse linear system solves. In Section 6, we summarize the performance assessment results and draw some preliminary conclusions on what performance we may achieve for sparse linear algebra on the A100 GPU.

We emphasize that with this paper, we do not intend to provide another technical specification of NVIDIA's A100 GPU, but instead focus on the reporting of performance we observe on this architecture for sparse linear algebra operations. Still, for convenience, we append a table from NVIDIA's whitepaper on the NVIDIA A100 Tensor Core GPU Architecture [20] that lists some key characteristics and compares against the predecessor GPU architectures. For further information on the A100 GPU,

we refer to the whitepaper [20], and encourage the reader to digest the performance results we present side-by-side with these technical details.

2 MEMORY BANDWIDTH ASSESSMENT

The performance of sparse linear algebra operations on modern hardware architectures is usually limited by the data access rather than compute power. In consequence, for sparse linear algebra, the performance-critical hardware characteristics are the memory bandwidth and the access latency. For main memory access, both metrics are typically somewhat intertwined, in particular on processors operating in streaming mode like GPUs. In this section, we assess the memory access performance by means of the Babel-STREAM benchmark [10].

We show the Babel-STREAM benchmark results for both an NVIDIA V100 GPU Figure 1a and an NVIDIA A100 GPU Figure 1b. The figures reflect a significant bandwidth improvement for all operations on the A100 compared to the V100. For an array of size 8.2 GB, the V100 reaches for all operations a performance between 800 and 840 GB/s whereas the A100 reaches a bandwidth between 1.33 and 1.4 TB/s.

In Figure 2, we present the data as a ratio between the A100 and V100 bandwidth performance for all operations. In Figure 2a, we show the performance ratio for increasing array sizes and observe the A100 providing a lower bandwidth than the V100 GPU for arrays of small size. For large array sizes, the A100 has a significantly higher bandwidth, converging towards a speedup factor of 1.7 for most memory access benchmarks, see Figure 2b.

3 SPARSE MATRIX VECTOR PRODUCT

The sparse matrix-vector product (SpMV) is a heavily-used operation in many scientific applications. The spectrum ranges from the power iteration [8], an iterative algorithm for finding eigenpairs in Google's Page Rank algorithm [16], to iterative linear system solvers like Krylov solvers that form the backbone

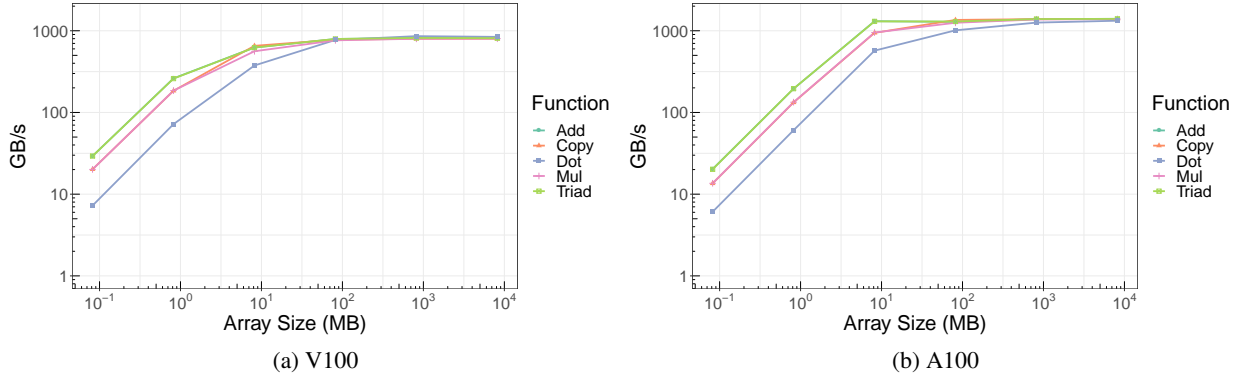


Figure 1: Performance of the Babel-STREAM benchmark on both V100 and A100 NVIDIA GPUs.

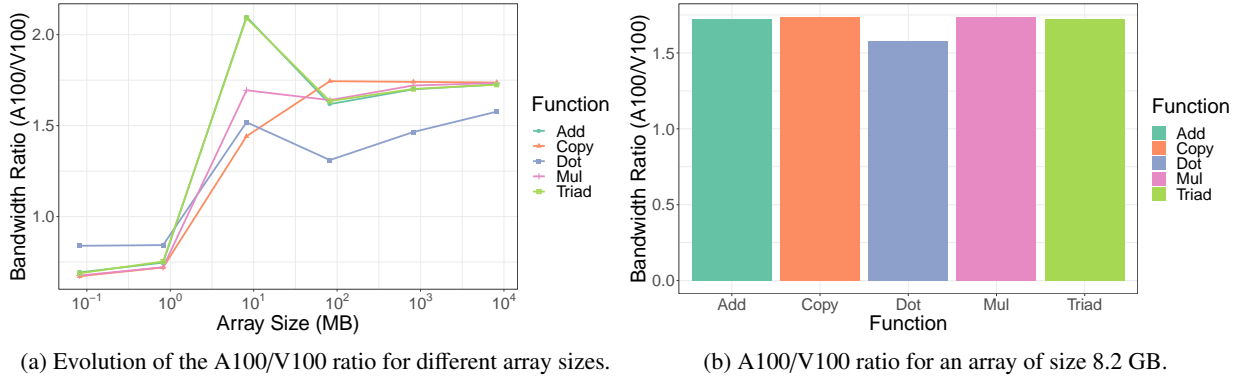


Figure 2: Ratio of the performance improvement of A100 compared to V100 NVIDIA GPUs for the Babel-STREAM benchmark.

of many finite element simulations. Given this importance, we put particular focus on the performance of the SpMV operation on NVIDIA’s A100 GPU. However, the performance not only depends on the hardware and the characteristics of the sparse matrix but also the specific SpMV format and processing strategy. Generally, all SpMV kernels aim at reducing the memory access cost (and computational cost) by storing only the nonzero matrix values [6]. Some formats additionally store a moderate amount of zero elements to enable faster processing when computing matrix-vector products [7]. But independent of the specific strategy, since SpMV kernels store only a subset of the elements, they share the need to accompany these values with information that allows to deduce their location in the original matrix [3]. We here recall in Figure 3 some widespread sparse matrix storage formats and kernel parallelization techniques.

A straightforward idea is to accompany the nonzero elements with the respective row and column indexes. This storage format, known as coordinate (COO [6]) format, allows determining the original position of any element in the matrix without processing other entries, see first row in Figure 3. A standard parallelization of this approach assigns the matrix rows to the distinct processing elements (cores). However, if few rows contain a significant portion of the overall nonzeros, this can result in a significant imbalance of the kernel and poor performance. A workaround is to distribute the nonzeros across the parallel resources, see the

right-hand side in Figure 3. However, as this can result in several processing elements contributing partial sums to the same vector output entry, sophisticated techniques for lightweight synchronization are needed to avoid write conflicts [11].

Starting from the COO format, further reduction of the storage cost is possible if the elements are sorted row-wise, and with increasing column-order in every row. (The latter assumption is technically not required, but it usually results in better performance.) Then, this Compressed Sparse Row (CSR [6]) format can replace the array containing the row indexes with a pointer to the beginning of the distinct rows, see the second row in Figure 3. While this generally reduces the data volume, the CSR format requires extra processing to determine the row location of a certain element. For a standard parallelization over the matrix rows, the row location is implicitly given, and no additional information is needed. However, similar to the COO format, better load balancing is available if parallelizing across nonzero elements. This requires the matrix row information and sophisticated atomic writes to the output vector [12].

A strategy that reduces the row indexing information even further is to pad all rows to the same number of nonzero elements and accompany the values only with the column indexes. In this ELL format [7] (third row in Figure 3), the row index of an element can be deduced from its location in the array storing the

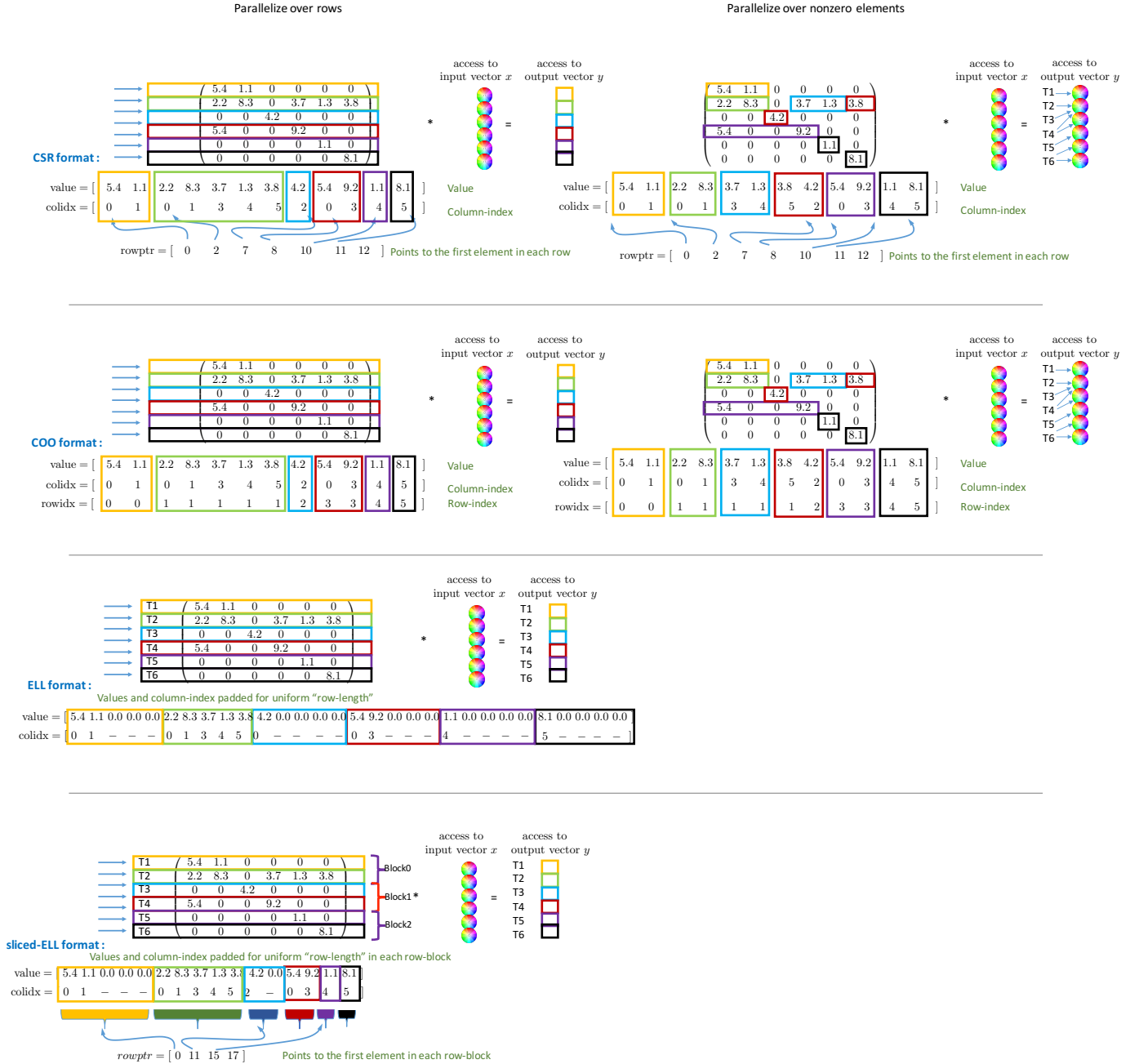


Figure 3: Overview over sparse matrix formats and SpMV kernel design.

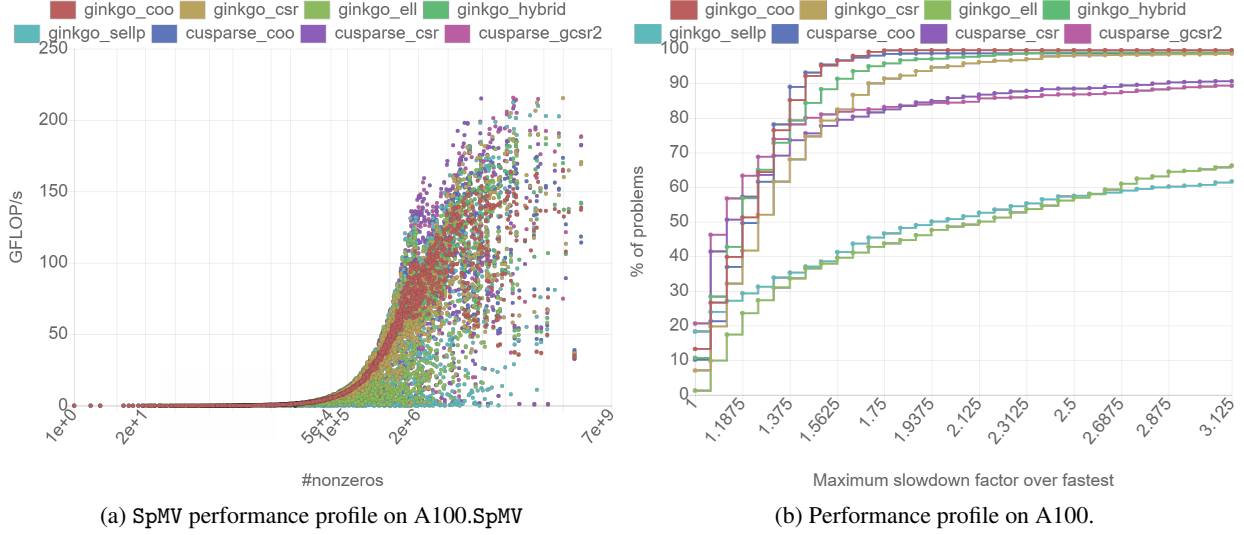


Figure 4: Left: SpMV kernel performance on the A100 GPU considering 2,800 test matrices from the Suite Sparse Matrix Collection. Right: Corresponding Performance profile for all SpMV kernels considered.

values in consecutive order and the information of how many elements are stored in each row. While this format is attractive for vector processors as it allows to execute in SIMD fashion with coalesced memory access, its efficiency heavily depends on the matrix characteristics: for well-balanced matrices, it optimizes memory access cost and operation count; but if one or a few rows contain much more nonzero elements than the others, ELL introduces a significant padding overhead and quickly becomes inefficient [3].

An attractive strategy to reduce the padding overhead the ELL format introduces for unbalanced matrices is to decompose the original matrix into blocks containing multiple rows, and to store the distinct blocks in ELL format. Rows of the same block contain the same number of nonzero elements, rows in distinct blocks can differ in the number of nonzero elements. In this Sliced ELL format (SELL [15], see the fourth row in Figure 3), the row pointer can not completely be omitted like in the ELL case, but a row pointer to the beginning of every block is needed. In this sense, the SELL format is a trade-off between the ELL format on the one side and the CSR format on the other side. Indeed, choosing a block size of 1 results in the CSR format, choosing a block size of the matrix size results in the ELL format. In practice, the block size is adjusted to the matrix properties and the characteristics of the parallel hardware, i.e. SIMD-width [5].

Another strategy to balance between the effectiveness of the ELL SpMV kernel and the more general CSR/COO SpMV kernels is to combine the formats in a “hybrid” SpMV kernel [3]. The concept behind is to store the balanced part of the matrix in ELL format and the unbalanced part in CSR or COO format. The SpMV operation then invokes two kernels, one for the balanced part and one for the unbalanced part.

For all these SpMV kernel strategies, there has been significant research efforts to optimize their performance on GPU architectures, see, e.g., [3, 9, 18, 17, 14, 21] and references therein. We here focus on the SpMV kernels of the cuSPARSE and Ginkgo

libraries that are well-known to belong to the most efficient implementations available.

4 SpMV PERFORMANCE ASSESSMENT

For the SpMV kernel performance assessment, we consider more than 2,800 matrices from the Suite Sparse Matrix collection [22]. Specifically, we consider all real matrices except for Figure 4b where we require the matrix to contain more than 1e5 nonzero elements. On the A100 GPU, we run the SpMV kernels from NVIDIA’s cuSPARSE library in version 11.0 (Release Candidate) and the Ginkgo open source library version 1.2 [2]. On the older V100 GPU, we run the same version of the Ginkgo library but use the cuSPARSE version 10.1¹.

On the left-hand side of Figure 4, we initially show the performance of all considered SpMV kernels on the A100 GPU for all test matrices: each dot represents the performance one of the SpMV kernels achieves for one test matrix. While it is impossible to draw strong conclusions, we can observe some CSR-based SpMV kernels exceed 200 GFLOP/s. This is consistent with the roofline model [23]: if we assume every entry of a CSR matrix needs 12 bytes (8 bytes for the fp64 values, 4 bytes for the column index, and ignoring the row pointer), assume all vector entries are cached (ignoring access to the input and output vectors), and a peak memory bandwidth of 1.4TB/s, we end up with $2nnz \cdot \frac{1.400GB/s}{12B/nnz} \approx 230GFLOP/s$.

On the right-hand side of Figure 4, we show a performance profile [13] considering all SpMV kernels available in either cuSPARSE or Ginkgo for real matrices containing more than 1e5 nonzero elements. As we can see, the cusparse_gcsr2 kernel has the largest share in terms of being the fastest kernel for a problem. However, cusparse_gcsr2 does not generalize well: cusparse_gcsr2 is more than 1.5× slower than the fastest ker-

¹cusparse_csr and cusparse_coo are part of CUDA version 11.0, CUDA 10.1 contains the conventional CSR SpMV routine

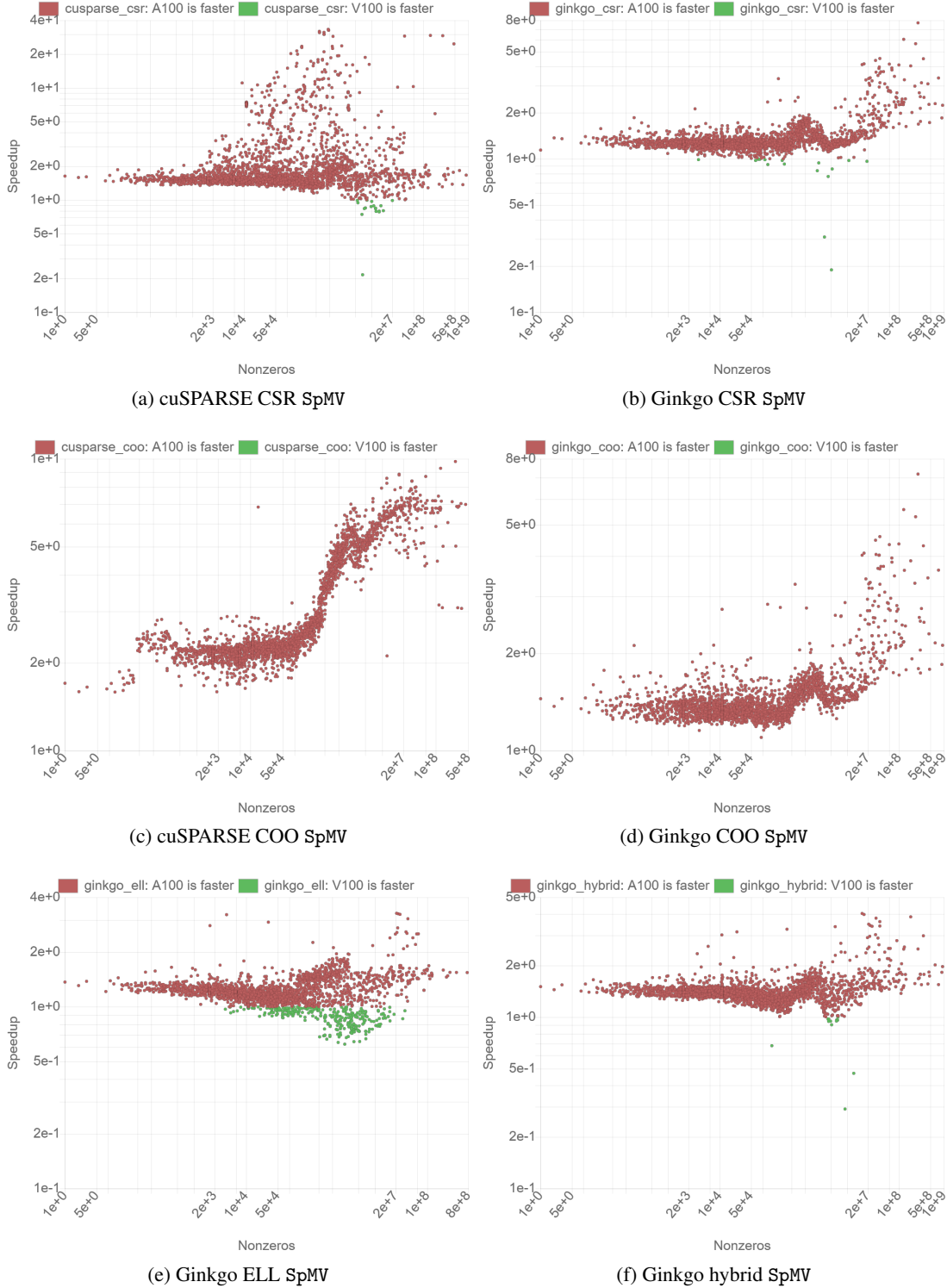


Figure 5: Performance improvement assessment of the A100 GPU over the V100 GPU for SpMV kernels from NVIDIA’s cuSPARSE library and Ginkgo.

nel for 20% of the problems, and more than $3\times$ slower than the fastest kernel for 10% of the problems. Although Ginkgo CSR SpMV kernel is not the fastest choice for as many problems as the `cusparse_csr` and the `cusparse_gcsr2` kernels,

Ginkgo CSR generalizes better, and virtually never more than $2.5\times$ slower than the fastest kernels among all matrices. The kernels providing the best performance portability across all matrix problems are the COO SpMV kernels from Ginkgo and

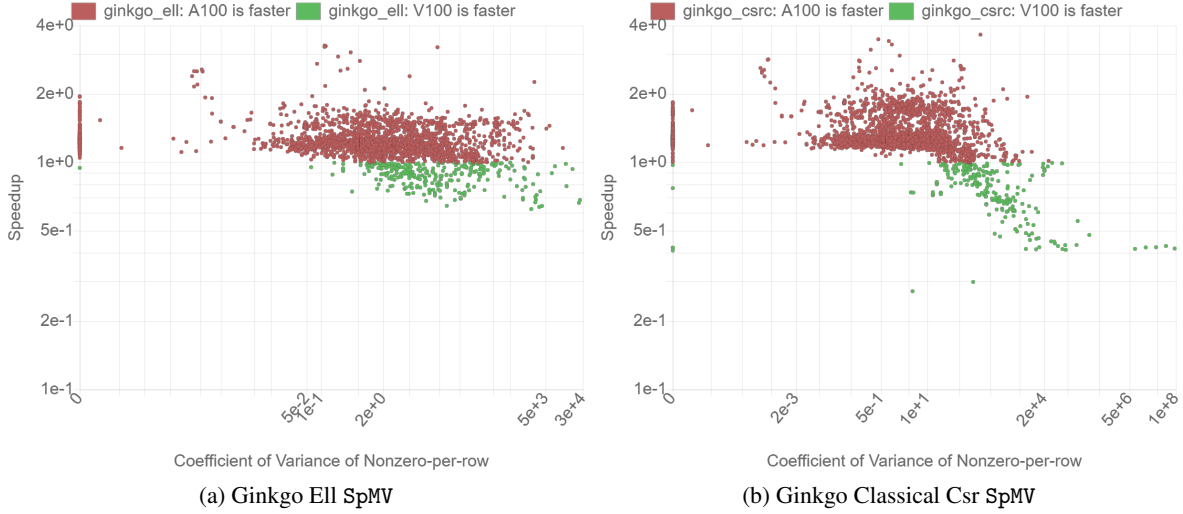


Figure 6: Performance improvement of the A100 GPU over the V100 GPU for Ell and Classical Csr from Ginkgo with coefficient of variance of nonzero-per-row.

cuSPARSE: only for 10% of the problems are they more than $1.4\times$ slower than the fastest kernel. As expected, the SELLP SpMV kernel does not generalize well, but it is the fastest kernel for 20% of the problems.

We then evaluate the performance improvements when comparing the SpMV kernels on the newer NVIDIA A100 GPU and the older NVIDIA V100 GPU. In Figure 5, we visualize the speedup factors for NVIDIA’s cuSPARSE library (left-hand side) and the Ginkgo library (right-hand side). In the first row of Figure 5 we focus on the CSR performance. As expected, the CSR SpMV achieves higher performance on the newer A100 GPU. For both libraries, cuSPARSE and Ginkgo, the CSR kernels achieve for most matrices a $1.7\times$ speedup on the A100 GPU – which reflects the bandwidth increase. However, for many matrices, the speedup exceeds $1.7\times$. For Ginkgo, the acceleration of up to $8\times$ might be related to larger caches on the A100 GPU allowing for more efficient caching of the input vector entries. The even larger speedups of up to $40\times$ for the cuSPARSE CSR kernel are likely only in part coming from the newer hardware: cuSPARSE 11.0 introduces new sparse linear algebra kernels (generic API) that are different in design and interface compared to cuSPARSE 9.10.2 traditional kernels [19]. The analysis of the performance improvement for the COO kernels is presented in the second row of Figure 5. For matrices with less than 500,000 nonzeros, the performance improvements are about $1.3\times$ for the Ginkgo library and $2.1\times$ for the cuSPARSE library. For matrices with more than 500,000 nonzero elements, we observe a sudden increase of the speedup to $> 5\times$ for the cuSPARSE COO kernel, which is likely linked to an algorithm improvement. In the third row of Figure 5, we visualize the performance improvements for Ginkgo’s ELL and hybrid formats that do not have a direct counterpart in cuSPARSE 11.0. Again, we see that the A100 provides for most matrices about $1.4\times$ higher performance, however, especially for the ELL SpMV kernel, there are several matrices where the V100 achieved higher performance.

To investigate these singularities further, we correlate the performance improvement in Figure 6 to the coefficient of variance

of the nonzero-per-row metric – that is the ratio between the variance of the nonzero-per-row metric and the mean of the nonzero-per-row metric. Given the strategy Ginkgo’s ELL kernel balances the work, larger coefficient of variance tend to introduce small data reads that perform poorly on the A100 GPU. Even more visible is this effect for the CSR_C SpMV kernel, the classical row-parallelized CSR SpMV kernel, see the right-hand side in Figure 6: Irregular sparsity patterns resulting in frequent loads of small data arrays and reflected in large coefficient of variance result in poor performance of the A100 GPU. Remarkably, the V100 can better deal with the frequent access to small data arrays. Ginkgo’s CSR SpMV automatically chooses between the classical CSR_C kernel providing good performance for regular sparsity patterns and the load-balancing CSR_I kernel [12] providing good performance for unbalanced sparsity patterns.

5 KRYLOV SOLVER PERFORMANCE ASSESSMENT

Krylov methods are among the most efficient algorithms for solving large and sparse linear systems. When applied to a linear system $Ax = b$ (with the sparse coefficient matrix A , right-hand side b , and unknown x) Krylov solvers started with an initial guess x_0 produce a sequence of vectors x_1, x_2, x_3, \dots that, in general, progressively reduce the norm of the residuals $r_k = b - Ax_k$, eventually yielding an acceptable approximation to the solution of the system [4].

Algorithmically, every iteration of a Krylov solver is composed of a (sparse) matrix vector product to generate the new search direction, an orthogonalization procedure, and the update of the approximate solution and the residual vector. In practice, Krylov methods are often enhanced with preconditioners to improve robustness and convergence [4]. Ignoring the preconditioner, every iteration can be composed of level-1 BLAS routines (vector operations) and a level-2 BLAS in the form of a sparse matrix vector product (SpMV). All these components – and in virtually

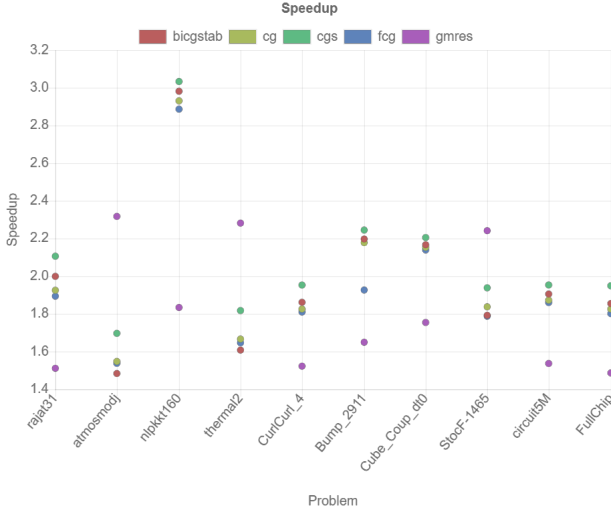


Figure 7: Krylov solver acceleration when upgrading from the V100 GPU to the A100 GPU.

all cases also the preconditioner application – are memory bound operations.

When upgrading from the V100 to the A100 GPU, for the vector updates and reduction operations, we can expect performance improvements corresponding to the bandwidth improvements observed in Section 2. For the basis-generating SpMV kernel, the improvements are problem-dependent and may even exceed the $1.7\times$ bandwidth improvement, see Section 4. The total solver speedup then depends on how the Krylov method composes the SpMV and vector operations, and how these components contribute to the overall runtime.

In Figure 7, we visualize the performance improvement observed when upgrading from the V100 to the A100 GPU. We select 10 test matrices that are large in terms of size and nonzero elements, different in their characteristics and representative for different real-world applications. The Krylov solvers are all taken from the Ginkgo library [2], the SpMV kernel we employ inside the solvers is Ginkgo’s COO SpMV kernel. For most test problems, we actually observe larger performance improvements than what the bandwidth ratios suggest. We also observe that if focusing exclusively on a single test problem, the speedup factors for the Krylov methods based on short recurrences (i.e. bicg, cg, cgs, fcg) are all almost identical. These methods are all very similar in design, and the SpMV kernel takes a similar runtime fraction. The gmres algorithm is not based on short recurrences but builds up a complete search space, and every new search direction has to be orthogonalized against all previous search directions. As this increases the cost of the orthogonalization step – realized via a classical Gram-Schmidt algorithm – the SpMV accounts for a smaller fraction of the algorithm runtime. As a result, the speedup for gmres is often different than the speedup for the other methods. However, also for gmres the speedup can exceed the $1.7\times$ bandwidth improvement as the A100 features larger caches that can be a significant advantage for the orthogonalization kernel. Overall, we observe that for most scenarios we tested, the Krylov solver executes on the A100 GPU more than $1.8\times$ faster than on the V100 GPU.

6 CONCLUSION

In this paper, we assessed the performance NVIDIA’s new A100 GPU achieves for sparse linear algebra operations. As most of these algorithms are memory bound, we initially present results for the STREAM bandwidth benchmark, then provide a very detailed assessment of the sparse matrix vector product performance for both NVIDIA’s cuSPARSE library and the Ginkgo open source library, and ultimately run complete Krylov solvers combining vector operations with sparse matrix vector products and orthogonalization routines. Compared to the predecessor, the A100 GPU provides a $1.7\times$ higher memory bandwidth, achieving almost 1.4 TB/s for large input sizes. The larger caches on the A100 allow for even higher performance improvements in complex applications like the sparse matrix vector product. Ginkgo’s Krylov iterative solver run in most cases more than $1.8\times$ faster on the A100 GPU than on the V100 GPU.

ACKNOWLEDGMENTS

This work was supported by the “Impuls und Vernetzungsfond” of the Helmholtz Association under grant VH-NG-1241 and by the Exascale Computing Project (17-SC-20-SC), a collaborative effort of the U.S. Department of Energy Office of Science and the National Nuclear Security Administration. The authors would like to thank the Steinbuch Centre for Computing (SCC) of the Karlsruhe Institute of Technology for providing access to an NVIDIA A100 GPU.

REFERENCES

- [1] The Top 500 List, <http://www.top.org/>.
- [2] Hartwig Anzt, Terry Cojean, Goran Flegar, Fritz Göbel, Thomas Grützmacher, Pratik Nayak, Tobias Ribizel, Yuh-siang Mike Tsai, and Enrique S. Quintana-Ortí. Ginkgo: A modern linear operator algebra framework for high performance computing, 2020.
- [3] Hartwig Anzt, Terry Cojean, Chen Yen-Chen, Jack Dongarra, Goran Flegar, Pratik Nayak, Stanimire Tomov, Yuh-siang M. Tsai, and Weichung Wang. Load-Balancing Sparse Matrix Vector Product Kernels on GPUs. *ACM Trans. Parallel Comput.*, 7(1), March 2020.
- [4] Hartwig Anzt, Mark Gates, Jack Dongarra, Moritz Kreutzer, Gerhard Wellein, and Martin Köhler. Preconditioned Krylov solvers on GPUs. *Parallel Computing*, 68:32–44, oct 2017.
- [5] Hartwig. Anzt, Stanimire. Tomov, and Jack. Dongarra. Implementing a Sparse Matrix Vector Product for the SELL-C/SELL-C- σ formats on NVIDIA GPUs. Technical Report ut-eecs-14-727, University of Tennessee, March 2014.
- [6] Richard. Barrett, Michael. Berry, Tony. F. Chan, James. Demmel, June. Donato, Jack. Dongarra, Viktor. Eijkhout, Roldan. Pozo, Charles. Romine, and Henk. Van der Vorst. *Templates for the Solution of Linear Systems: Building Blocks for Iterative Methods, 2nd Edition*. SIAM, Philadelphia, PA, 1994.

- [7] Nathan Bell and Michael Garland. Implementing sparse matrix-vector multiplication on throughput-oriented processors. In *Proceedings of the Conference on High Performance Computing Networking, Storage and Analysis*, SC ’09, pages 18:1–18:11, New York, NY, USA, 2009. ACM.
- [8] Gianna M. Del Corso. Estimating an eigenvector by the power method with a random start. *SIAM J. Matrix Anal. Appl.*, 18(4):913–937, October 1997.
- [9] Steven. Dalton, Sean. Baxter, Duane. Merrill, Luke. Olson, and Michael. Garland. Optimizing sparse matrix operations on gpus using merge path. In *2015 IEEE International Parallel and Distributed Processing Symposium*, pages 407–416, May 2015.
- [10] Tom Deakin, James Price, Matt Martineau, and Simon McIntosh-Smith. Gpu-stream v2.0: Benchmarking the achievable memory bandwidth of many-core processors across diverse parallel programming models. In Michela Taufer, Bernd Mohr, and Julian M. Kunkel, editors, *High Performance Computing*, pages 489–507, Cham, 2016. Springer International Publishing.
- [11] Goran Flegar and Hartwig Anzt. Overcoming load imbalance for irregular sparse matrices. In *Proceedings of the Seventh Workshop on Irregular Applications: Architectures and Algorithms*, IA3’17, pages 2:1–2:8, New York, NY, USA, 2017. ACM.
- [12] Goran Flegar and Enrique S. Quintana-Ortí. Balanced csr sparse matrix-vector product on graphics processors. In Francisco F. Rivera, Tomás F. Pena, and José C. Cabaleiro, editors, *Euro-Par 2017: Parallel Processing*, pages 697–709, Cham, 2017. Springer International Publishing.
- [13] Nicholas Gould and Jennifer Scott. A note on performance profiles for benchmarking software. *ACM Trans. Math. Softw.*, 43(2), August 2016.
- [14] Changwan Hong, Aravind Sukumaran-Rajam, Israt Nisa, Kunal Singh, and P. Sadayappan. Adaptive sparse tiling for sparse matrix multiplication. In *Proceedings of the 24th ACM SIGPLAN Symposium on Principles and Practice of Parallel Programming, PPoPP 2019, Washington, DC, USA, February 16-20, 2019*, pages 300–314, 2019.
- [15] Moritz Kreutzer, Georg Hager, Gerhard Wellein, Holger Fehske, and Alan R. Bishop. A unified sparse matrix data format for efficient general sparse matrix-vector multiplication on modern processors with wide SIMD units. *SIAM J. Scientific Computing*, 36(5):C401–C423, 2014.
- [16] Amy N. Langville and Carl D. Meyer. *Google’s PageRank and Beyond: The Science of Search Engine Rankings*. Princeton University Press, Princeton, NJ, USA, 2012.
- [17] Duane Merrill and Michael Garland. Merge-based parallel sparse matrix-vector multiplication. In *Proceedings of the International Conference for High Performance Computing, Networking, Storage and Analysis*, SC ’16, pages 58:1–58:12, Piscataway, NJ, USA, 2016. IEEE Press.
- [18] Duane Merrill, Michael Garland, and Andrew S. Grimshaw. High-performance and scalable GPU graph traversal. *TOPC*, 1(2):14:1–14:30, 2015.
- [19] NVIDIA. CUDA 11.0 Release Notes. <https://docs.nvidia.com/cuda/cuda-toolkit-release-notes/index.html#title-new-features>, 06 2020.
- [20] Nvidia. NVIDIA A100 Tensor Core GPU Architecture. <https://www.nvidia.com/content/dam/en-zz/Solutions/Data-Center/nvidia-ampere-architecture-whitepaper.pdf>, June 2020.
- [21] Lawrence. Page, Sergey. Brin, Rajeev. Motwani, and Terry. Winograd. The PageRank citation ranking: Bringing order to the Web. In *Proceedings of the 7th International World Wide Web Conference*, pages 161–172, Brisbane, Australia, 1998.
- [22] SuiteSparse. Matrix Collection. <https://sparse.tamu.edu>, 2018. Accessed in April 2018.
- [23] Samuel Williams, Andrew Waterman, and David Patterson. Roofline: An Insightful Visual Performance Model for Multicore Architectures. *Commun. ACM*, 52(4):65–76, April 2009.

Features	V100	A100
GPU Architecture	NVIDIA Volta	NVIDIA A100
SMs	80	108
TPCs	40	54
FP32 Cores/SM	64	64
FP64 Cores/SM	32	32
INT32 Cores/SM	64	64
GPU Boost Clock	1530 MHz	1410 MHz
Peak FP16 TFLOPS	31.4	78
Peak FP32 TFLOPS	15.7	19.5
Peak FP64 TFLOPS	7.8	9.7
Texture Units	320	432
Memory Interface	4096-bit HBM2	5120-bit HBM2
Memory Data Rate	877.5 MHz DDR	1215 MHz DDR
Memory Bandwidth	900 GB/sec	1555 GB/sec
L2 Cache	6144 KB	40960 KB
Shared Memory Size/SM	96 KB	164 KB
Register File Size	256 KB	256 KB
Transistors	21.1 billion	54.2 billion

Table 1: Technical characteristics of NVIDIA’s V100 and A100 GPU architecture in comparison to its predecessors [20].